Alteration Pattern and Fluid Inclusions of Gold-Bearing Quartz Veins in Archean Trondhjemite near Wawa, Ontario, Canada

PAUL A. STUDEMEISTER

Portland Cement Association, 5420 Old Orchard Road, Skokie, Illinois 60077-4321

AND STEPHANOS KILIAS

Geologisk Centralinstitut, Øster Voldgade 10, DK-1350 København K, Denmark

Abstract

Systems of auriferous quartz veins occur in Archean granitic rocks within 1.6 km of the Wawa greenstone belt, 80 km northeast of Wawa, Ontario. The vein system at the Renabie mine strikes west for approximately 850 m, dips steeply to a depth of at least 950 m, and hosts orebodies up to 30 m wide and 210 m long. The six vein systems at the Braminco prospect strike north to northwest, dip steeply, and are up to 20 m wide. Alteration of feldspar to quartz + calcite + white mica + albite, and of biotite + amphibole to chlorite, intensifies within 2 to 4 m of quartz vein systems bearing native gold. Mass balance calculations suggest that the alteration of granitic rocks added K, CO_2 + H_2O, Rb, and Ba and removed Na.

Three types of primary fluid inclusions coexist in quartz from the auriferous vein systems. Type I, the most abundant type, is an aqueous solution with 10 to 25 vol percent CO_2 with density of 0.75 g/cm^3; homogenization temperatures range from 220° to 360°C. Type II is nearly 100 vol percent liquid CO_2, with a density of 0.95 g/cm^3. Type III, the least abundant type, is an aqueous liquid with 10 to 50 vol percent H_2O gas; homogenization temperatures range from 120° to 220°C. Apparent salinities of types I, II, and III, based on clathrate and ice melting points, are estimated to be 4 to 8, 0, and 11 to 14 equiv wt percent NaCl, respectively.

The preferred interpretation is that the gold-bearing quartz veins formed from CO_2-laden fluids of less than 10 equiv wt percent NaCl during regional greenschist metamorphism of granitic rocks. The three types of fluid inclusions may represent two or three different generations of fluids trapped over a range of temperature and pressure. Another possibility is that the fluid inclusions represent samples of a fluid comprised of immiscible CO_2 and NaCl-H_2O phases, entrapped during quartz crystallization. The source of the gold is not known.

Introduction

TWO features suggest that lode gold deposits in Archean greenstone belts of Canada formed from fluids of similar composition. First, alteration halos around many deposits have minerals in common such as quartz, white mica, carbonate minerals, pyrite, and chlorite (Boyle, 1979; Hodgson and MacGeehan, 1982). Mass balance studies (Kerrich, 1981; Kerrich and Hodder, 1982) report that alteration added CO_2, Si, plus K to the host rocks and removed Na from them.

Second, fluid inclusion research suggests that the fluids contained carbon dioxide and less than 10 equiv wt percent NaCl. Kerrich and Hodder (1982) report 0.5 to 2.6 equiv wt percent NaCl in fluid inclusions from the Con mine, Yellowknife district, and the Lamaque mine, Cadillac district. The McIntyre-Hollinger deposit, Timmins district, reportedly has CO_2-laden fluid inclusions with salinities not exceeding 2 equiv wt percent NaCl (Smith et al., 1984). Guha et al. (1982) report clathrate melting points for CO_2-laden inclusions in quartz from the Doyon mine, Bousquet district, that correspond to less than 6 equiv

wt percent NaCl. Walsh et al. (1984) interpret 1.5 to 3.5 equiv wt percent NaCl for fluid inclusions in quartz from the Porcupine district.

This paper discusses the alteration pattern and fluid inclusions of auriferous quartz vein systems in the Renabie mine area, Michipicoten district, 80 km northeast of Wawa, Ontario (Fig. 1). The Renabie mine produced 33 million metric tons of ore averaging 7.89 g/metric ton Au between 1947 and 1970 (Tintor, 1984). The vein systems are mainly in granitic rocks of Archean age intruding the Wawa greenstone belt. The Wawa greenstone belt is an Archean sequence of three main cycles of felsic to mafic volcanic rocks (Attoh, 1980; Sage, 1981) metamorphosed in the regional greenschist to amphibolite facies.

Methodology

Samples were collected along three traverses, each 2 to 3 m long, across the granitic wall rocks of two vein systems in the area (Fig. 2). Two of the traverse suites are from the vein system hosting the Renabie mine: suite A is from the C zone at the surface and suite B is from the 3,100-ft (914-m) level under-
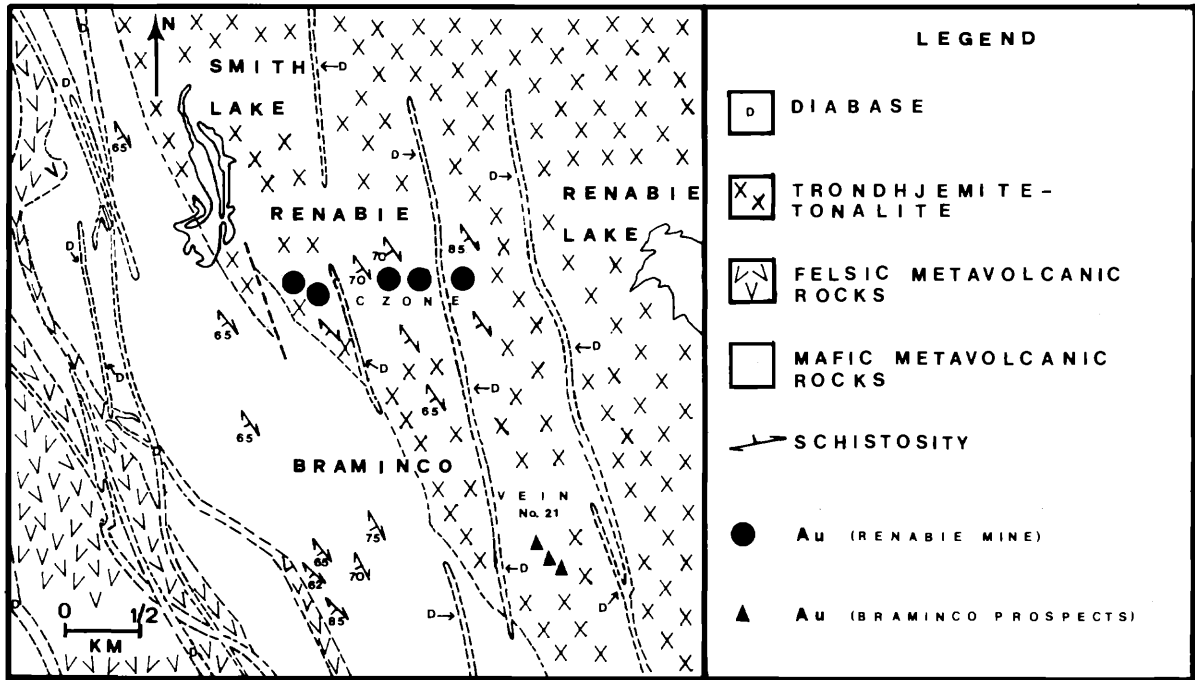
FIG. 1.   Geology of the Renabie area, Leeson Township, Sudbury district, Ontario, Canada.

ground. Suite C is from the surface exposure of the No. 21 vein system at the Braminco prospect. Samples of quartz for fluid inclusion study were selected from veins at the surface C zone and underground at the 3,100-ft (914-m) and 1,250-ft (458-m) levels of the Renabie mine. The No. 21 vein system was also sampled for quartz.

The research was carried out in the laboratories of the University of Ottawa, Ottawa, Ontario (Kilias,

FIG. 2.   Location of samples for geochemical analysis.

1984). Thin sections of samples were studied under a polarizing-light microscope to determine mineralogy and microstructure. X-ray diffraction analysis of powdered samples complemented the petrographic study. Fusion disks and pressed pellets of powdered samples were analyzed for major and some trace elements with an X-ray fluorescence spectrometer.

A Linkam TH 600 microthermometric system (Shepherd, 1981) equipped with a heating-freezing stage was used to study fluid inclusions in quartz samples. The heating-freezing stage was calibrated between −95° and +398°C, following the method of MacDonald and Spooner (1981). Isolated inclusions, lacking evidence of secondary origin by criteria in Roedder (1979), were presumed to be of primary origin and subject to research. Fluid inclusions were classified on the basis of phase relations observed at room temperature.

Alteration Pattern

The gold-bearing quartz vein systems are in Archean granitic rocks within 1.6 km of the intrusive contact with the Wawa greenstone belt (Fig. 1). The granitic rocks are massive to foliated, leucocratic assemblages of feldspar, quartz, biotite, and amphibole of hornblende to actinolite composition. Minor minerals are white mica, calcite, epidote, chlorite, pyrite, sphene, magnetite, apatite, and zircon. According to the nomenclature of Ayres (1972), granitic rocks are termed trondhjemite or tonalite because
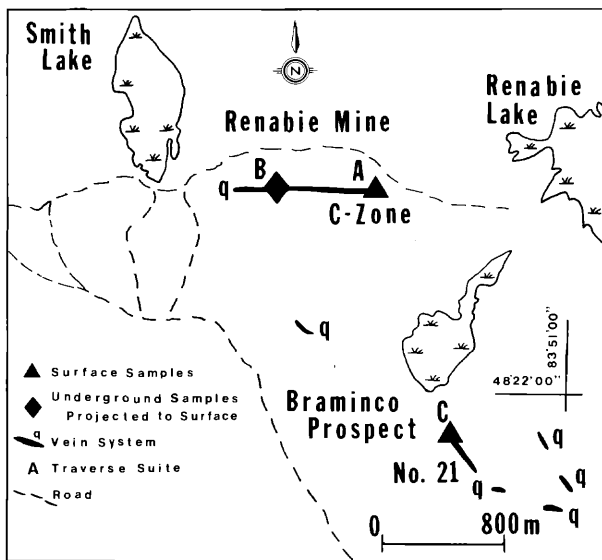
the modal ratio of potash feldspar to plagioclase is less than 1/5; the plagioclase is of albite to oligoclase composition. Mafic metavolcanic rocks in and adjacent to the granitic rocks are mainly assemblages of amphibole (hornblende, actinolite), epidote, plagioclase (albite, oligoclase), chlorite, biotite, and quartz. Minor minerals observed are calcite, ferrodolomite, white mica, sphene, magnetite, apatite, pyrite, and chalcopyrite.

Textural relations suggest that the granitic and mafic metavolcanic rocks were affected by regional metamorphism to the greenschist facies. Feldspars are variably altered to combinations of fine white mica, calcite, epidote, and albite. Chlorite with or without sphene is partly or wholly pseudomorphous after biotite. Amphibole is partly replaced by mixtures of fine chlorite, calcite, and quartz; and some epidote is altered to calcite and chlorite. Many amphibole grains have interiors of dark green hornblende and irregular rims of pale green actinolite with chlorite.

Quartz vein systems

Chlorite + white mica + albite + calcite + quartz alteration of granitic rocks intensifies within 2 to 4 m of quartz vein systems. A quartz vein system generally consists of lensoidal quartz veins and fragments of wall rock enveloped by a foliated matrix of quartz, calcite, white mica, albite, and chlorite. En echelon arrangement of the quartz veins and wall-rock enclaves, more or less parallel to the matrix foliation, imparts a banded structure. Quartz vein systems are considered to be metamorphogenic fractures filled with minerals and fringed by altered rocks.

The vein system hosting the Renabie mine is in granitic rocks, varies 1 to 30 m in width, strikes west for approximately 850 m, and dips steeply to a depth of at least 950 m. Orebodies, up to 30 m wide and 210 m long, are mixtures of vein and matrix material bearing pyrite with minor amounts of galena, chalcopyrite, sphalerite, molybdenite, and native gold. Traces of tellurobismuthite (Bi_2Te_3), altaite (PbTe), hessite (Ag_2Te), petzite (Ag_3AuTe_2), and rucklidgeite ($(Bi,Pb)_3Te_4$) also occur. At the Braminco prospect, native gold occurs with similar gangue minerals in six different vein systems traversing granitic and mafic metavolcanic rocks. The vein systems at the surface are up to 20 m wide, strike north to northwest, and dip steeply to an unknown depth.

Petrographic study of traverse suites A, B, and C indicates mineral alteration of granitic rocks with proximity to vein systems: (1) feldspars become more sodic in composition; (2) content of white mica plus calcite increases at the expense of feldspar; (3) content of chlorite increases at the expense of biotite, amphibole, and epidote; and (4) foliation, is enhanced.

Mass balance

Simple comparison of the bulk chemical analysis of granitic rocks and alteration products is not satisfactory for deducing chemical changes resulting from hydrothermal alteration. During the alteration of rock the abundance of a chemical component may change by real gain or loss, dilution with addition of other components, concentration with leaching of soluble components, or change in rock volume. The mass balance equation of Gresens (1967) calculates real gains and losses, taking into account possible changes in rock volume and specific gravity.

Let us consider a granitic rock, initially a = 100 g, transformed into an alteration product by hydrothermal fluids. The gain or loss in the abundance of component i, ΔX_i, is according to Gresens (1967):

$$\Delta X_i = a((Fy_i\beta/\sigma) - x_i), \qquad (1)$$

where x_i and y_i are the weight fractions of component i in granitic rock and alteration product, respectively; β and σ are the specific gravities of alteration product and granitic rock, respectively; and F is the volume factor, the ratio between final and initial volume of rock.

If the chemical compositions and specific gravities are known from laboratory analysis, then a unique solution to equation (1) is found by defining a value for the volume factor. The volume factor is defined by first establishing the immobile behavior of two or more components, and then solving equation (1) for F by substituting $\Delta X = 0$ for the immobile components (Gresens, 1967). Two components are considered immobile if ratios to one another are constant in a suite of rocks at different alteration intensities.

The chemical changes in the hydrothermal alteration of granitic rocks are deduced by the Gresens (1967) method. Each of the traverse suites A, B, and C consists of rocks at different alteration intensities, which correlate with sampling distance from the vein system. The sample collected farthest from the vein system is least altered and the remaining samples in each suite are compared to it. The Al_2O_3 to TiO_2 ratios are approximately uniform in each suite (Table 1), suggesting that Al and Ti experienced little or no mobility during hydrothermal alteration. Hence, the volume factor for each comparison was estimated by solving equation (1) for F substituting $\Delta X(Al_2O_3) = 0$, repeating the calculations for TiO_2, and then taking the average of the two solutions. Results of mass balance calculations (Table 2) are plotted against sampling distance, and data points are joined by a curve. Net gain or loss of component i is estimated by integrating the area between $\Delta X_i = 0$ and the extrapolated curve (Figs. 3, 4, and 5).

All three suites suggest that alteration of the gra-

TABLE 1.   Chemical Composition of Traverse Suites A, B, and C

Sample number	Traverse A					Traverse B					Traverse C							
	16	17	20	21	25	125	126	127	128	129	59	62	63	64	65	66	67	69
Wt percent																		
SiO_2	65.14	64.04	64.41	61.95	57.70	70.68	69.86	71.63	68.81	71.12	72.51	70.32	70.37	71.04	68.69	67.51	72.09	75.18
Al_2O_3	16.17	14.45	15.52	14.47	15.46	14.37	14.85	14.83	13.84	14.76	15.38	14.49	15.23	14.12	14.94	16.73	15.61	14.51
Fe_2O_3	5.48	4.68	4.80	4.52	5.20	1.95	1.96	2.03	2.14	1.69	2.27	2.42	2.37	2.17	2.50	2.90	2.50	2.56
MgO	2.23	1.66	1.72	1.93	2.45	0.37	0.49	0.32	0.38	0.41	0.58	0.63	0.60	0.62	0.58	0.54	0.62	0.40
CaO	5.32	4.47	4.59	4.90	6.02	2.25	2.48	2.38	2.61	0.63	2.50	2.49	2.46	2.64	2.88	0.92	1.22	0.77
Na_2O	4.12	3.36	3.38	1.02	1.71	4.92	4.86	4.68	3.49	3.53	5.03	3.46	2.44	1.72	2.58	0.78	1.49	0.47
K_2O	0.92	1.31	1.51	4.41	4.48	1.51	1.34	1.58	2.73	3.17	1.50	2.74	3.62	4.20	3.61	5.41	4.56	4.69
TiO_2	0.52	0.45	0.48	0.52	0.49	0.18	0.19	0.19	0.19	0.19	0.27	0.25	0.26	0.24	0.26	0.29	0.26	0.25
P_2O_5	0.06	0.08	0.10	0.09	0.07	0.04	0.02	0.02	0.03	0.07	0.01	0.01	0.02	0.02	0.02	0.10	0.06	0.08
MnO	0.09	0.07	0.07	0.10	0.01	0.04	0.03	0.04	0.04	0.01	0.04	0.04	0.04	0.05	0.05	0.02	0.03	0.02
L.O.I.	0.80	4.80	2.71	5.70	6.00	3.46	3.95	3.14	4.91	5.90	0.91	2.62	2.97	3.34	3.49	4.00	2.50	2.61
Total	100.85	99.37	99.29	99.61	99.59	99.77	100.03	100.84	99.17	101.48	101.00	99.47	100.38	100.16	99.60	99.20	100.94	101.54
S	0.00	0.00	0.02	0.18	0.10	0.02	0.00	0.01	0.05	0.05	0.00	0.07	0.18	0.25	0.03	0.03	0.07	0.05
Ppm																		
Ba	252	354	422	913	543	350	387	553	451	603	503	466	459	462	482	656	564	992
Cr	35	12	56	2	53	23	8	23	25	40	5	9	3	0	0	28	10	23
Zr	136	139	170	144	133	85	136	86	88	68	117	113	112	121	120	111	118	97
Sr	263	275	364	327	294	341	376	313	217	271	278	203	259	229	282	200	221	191
Rb	7	28	35	127	129	41	17	35	77	82	28	65	99	109	94	142	125	122
Y	5	7	10	16	11	10	11	10	8	6	0	4	6	5	7	9	4	6
S.G.	2.77	2.74	2.76	2.77	2.78	2.70	2.72	2.73	2.73	2.72	2.69	2.70	2.69	2.73	2.72	2.77	2.73	2.79
(Al_2O_3/TiO_2)	31.0	32.1	32.3	27.9	31.5	79.8	78.2	78.0	72.8	77.7	56.9	58.0	58.5	58.8	57.5	57.7	60.0	58.0
Distance	2.5	1.9	1.4	0.5	0.0	2.5	1.9	1.4	0.5	0.0	2.5	2.1	1.9	1.6	1.4	1.1	0.5	0.0

Fe_2O_3 = total iron reported as Fe_2O_3; L.O.I. = volatiles (in wt %) lost on ignition at 1,000°C, uncorrected for oxidation of iron; S.G. = specific gravity; distance = distance (in m) of sample selection from the quartz vein system

TABLE 2. Results of Mass Balance Calculations, Traverse Suites A, B, and C

Sample pair	Traverse A				Traverse B				Traverse C						
	16→17	16→20	16→21	16→25	125→126	125→127	125→128	125→129	59→62	59→63	59→64	59→65	59→66	59→67	59→69
					(g/100 g of parent rock)										
SiO_2	7.71	2.89	31.50	−4.34	−1.01	−2.60	−7.37	9.56	−4.75	−7.07	−6.90	−10.00	−16.20	−5.93	1.57
Al_2O_3	0.27	0.22	6.40	0.12	0.44	−0.28	−1.64	2.28	−1.42	−1.22	−2.34	−1.78	−1.43	−0.96	−1.08
Fe_2O_3	−0.16	−0.41	1.57	0.00	0.01	−0.02	0.02	−0.04	0.06	−0.07	−0.27	0.01	0.15	0.04	0.25
MgO	−0.34	−0.41	0.78	0.35	0.12	−0.07	−0.02	0.09	0.03	−0.02	−0.01	−0.05	−0.13	−0.01	−0.19
CaO	−0.24	−0.47	2.32	0.97	0.22	0.01	0.15	−1.54	−0.10	−0.21	−0.06	0.12	−1.73	−1.37	−1.74
Na_2O	−0.30	−0.55	−2.53	−2.32	−0.07	−0.47	−1.71	−0.94	−1.70	−2.76	−3.44	−2.68	−4.38	−3.65	−4.57
K_2O	0.57	0.68	5.96	3.80	−0.17	−0.01	1.00	2.07	1.14	1.87	2.38	1.79	3.01	2.71	3.12
TiO_2	−0.01	−0.01	0.29	0.00	0.01	0.00	−0.01	0.03	−0.03	−0.03	−0.05	−0.03	−0.03	−0.03	−0.02
P_2O_5	0.03	0.05	0.08	0.01	−0.02	−0.02	−0.01	0.04	0.00	0.01	0.01	0.01	0.07	0.05	0.07
MnO	−0.01	−0.02	0.07	−0.08	−0.01	0.00	0.00	−0.03	0.00	0.00	0.01	0.01	−0.02	−0.01	−0.02
$L.O.I.$	4.66	2.06	8.09	5.52	0.48	−0.48	1.06	3.20	1.62	1.85	2.18	2.27	2.43	1.40	1.66
S	0.00	0.02	0.28	0.11	−0.02	−0.01	0.03	0.04	0.07	0.17	0.23	0.03	0.03	0.07	0.05
					(g/10⁶ g of parent rock)										
Ba	151	194	1,172	320	36	176	65	330	−54	−76	−76	−64	44	18	474
Cr	−21	24	−32	21	−15	−1	0	22	4	−2	−5	−5	18	4	18
Zr	22	44	89	4	51	−3	−4	−8	−8	−13	−5	−8	−24	−8	−21
Sr	50	122	247	47	34	−44	−141	−35	−82	−37	−67	−21	−111	−74	−90
Rb	25	30	191	129	−24	−8	30	52	35	64	73	58	90	87	92
Y	3	6	20	6	1	−1	−3	−3	4	6	5	6	8	4	6
F	1.15	1.06	1.56	1.05	0.99	0.94	0.91	1.12	0.96	0.93	0.91	0.90	0.81	0.91	0.95

Fe_2O_3 = total iron reported as Fe_2O_3; L.O.I. = volatiles lost on ignition at 1,000°C, uncorrected for oxidation of iron; F = volume factor: the average of the volume factors for Al_2O_3 and TiO_2, components assumed to be immobile
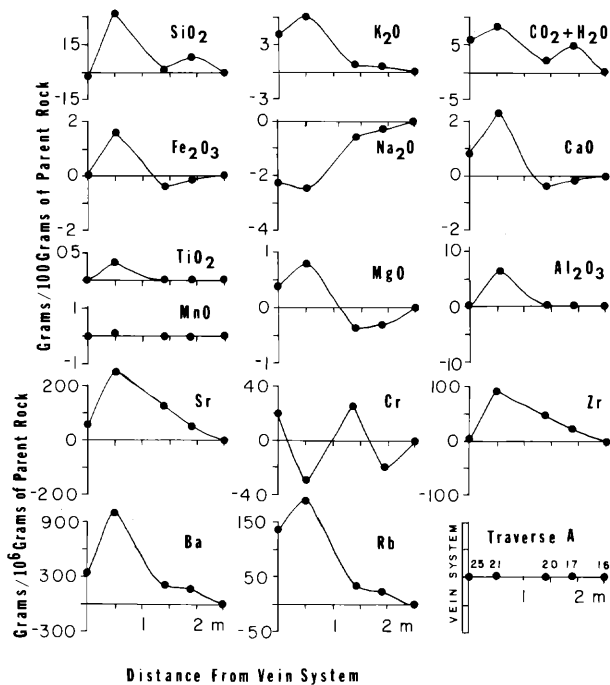
FIG. 3. Chemical alteration pattern for traverse suite A, C zone of the Renabie mine.

nitic rocks involved net gains of K, $CO_2 + H_2O$, Rb, and Ba and a net loss of Na (Figs. 3, 4, and 5). Gains of Rb and Ba, elements similar in ionic size and charge
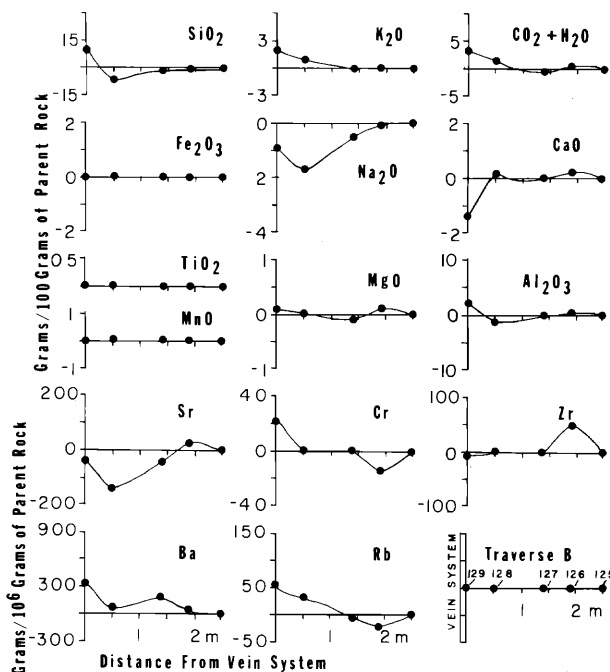

FIG. 4. Chemical alteration pattern for traverse suite B, 3,100-ft (914-m) level of the Renabie mine.
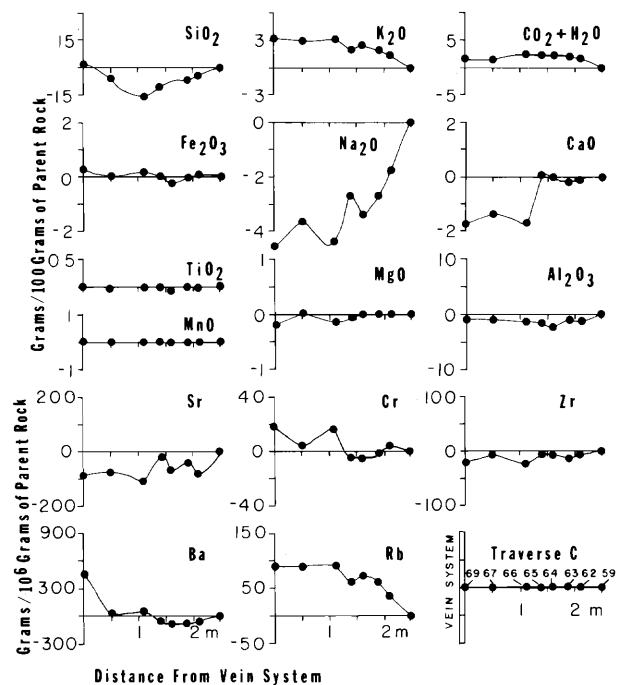

FIG. 5. Chemical alteration pattern for traverse suite C, No. 21 vein system of the Braminco prospect.

to K (Krauskopf, 1967), complement the abundance of white mica near the quartz vein systems. Loss of Na coupled with a gain of $CO_2 + H_2O$ is consistent with the alteration of feldspar to white mica and calcite.

Net changes in the remaining components are inconsistent in the three traverse suites (Figs. 3, 4, and 5). The calcium profile in suite A, for example, suggests that calcium was removed from the outer zone and added to the inner zone of the alteration halo. Profiles in suites B and C, however, suggest loss of calcium. One interpretation is that calcite, next in abundance to quartz in the vein systems, formed by reaction of CO_2, which was indigenous to the reactant fluid, with calcium released from the hydration of wall-rock feldspar. Studemeister (1983) reports similar alteration profiles for Ca and Mg in wall rocks to metamorphogenic quartz-carbonate veins around the Gutcher Lake stock, an Archean trondhjemite intrusion into the Wawa greenstone belt, 30 km north of Wawa. Another interpretation for inconsistent changes is that large variability in abundance masks possible gain or loss resulting from hydrothermal alteration.

Interpretation

The greenschist alteration of granitic rocks within 2 to 4 m of the quartz vein systems is interpreted as follows. A CO_2-H_2O fluid circulated along systems of

fractures during regional greenschist metamorphism in the Archean. The fluid deposited quartz along with native gold in the fractures, reacted with wall rocks to form albite + calcite + white mica from feldspar and chlorite from biotite + amphibole + epidote, added K, CO_2 + H_2O, Rb, and Ba, and leached Na. The alteration around the vein systems was fluid dominated, e.g., fluid/rock > 1, given that the wall rocks experienced mineral and chemical transformation.

The greenschist alteration of granitic rocks may be summarized by the following reaction:

$$40(0.9 \, NaAlSi_3O_8 + 0.1 \, CaAl_2Si_2O_8)$$
plagioclase

$$+ 1K_2(Mg,Fe)_5Al_4Si_5O_{20}(OH)_4 + 6H_2O$$
biotite   fluid

$$+ 4CO_2 + 2KCl \rightarrow 2K_2Al_6Si_6O_{20}(OH)_4$$
fluid   fluid   muscovite

$$+ 4CaCO_3 + 1(Mg,Fe)_5Al_2Si_3O_{10}(OH)_8$$
calcite   chlorite

$$+ 34NaAlSi_3O_8 + 4SiO_2 + 2NaCl. \qquad (2)$$
albite   quartz   fluid
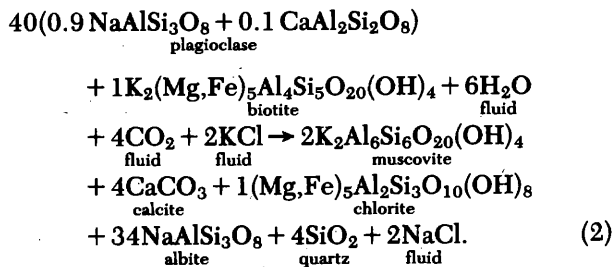
Gradients in fluid/rock and $X(CO_2)/X(H_2O)$ ratios probably influenced the intensity of greenschist alteration. Around fracture systems, large reactant fluid to rock volumes drove reaction (2) to the right, resulting in advanced alteration of mineral reactants. Away from fracture systems, small fluid to rock volumes prevailed and reaction (2) ceased when fluid reactants (e.g., CO_2, H_2O) were consumed. The result was partial alteration of mineral reactants. A simple correspondence between alteration intensity and gold tenor does not exist in the study area. Gold is concentrated in vein systems fringed by altered rocks, but not all vein systems with alteration are gold bearing.

Fluid Inclusions

Three types of primary fluid inclusions were observed in quartz from auriferous veins at the Renabie mine and Braminco prospect:

Type I: three-phase inclusions of an aqueous liquid with 10 to 25 vol percent, but occasionally 30 to 50 vol percent, liquid plus gas CO_2 (Fig. 6A). Top widths of inclusions were measured to be 9 to 30 μm.

Type II: one-phase inclusions of virtually 100 vol percent liquid CO_2 (Fig. 6B), and less frequently, two-phase inclusions of 70 to 90 vol percent liquid CO_2 and 10 to 30 vol percent H_2O. Water, where present, occurs as a film on the inner cavity wall. Type II inclusions occur with type I, and top widths were measured to be 6 to 25 μm. No temperature data were recorded for the two-phase inclusions.
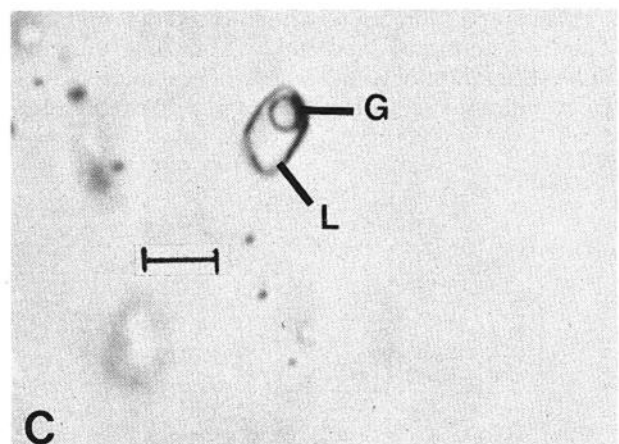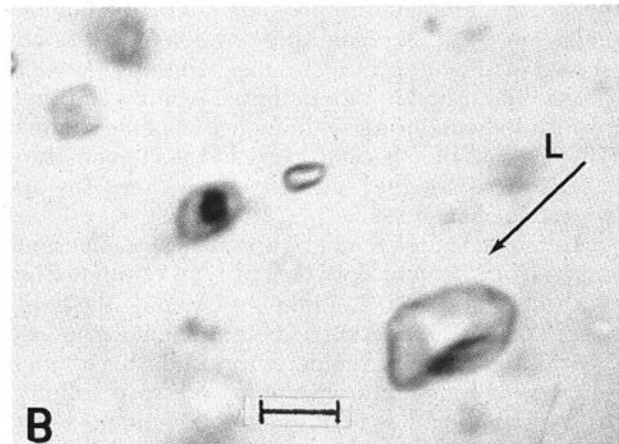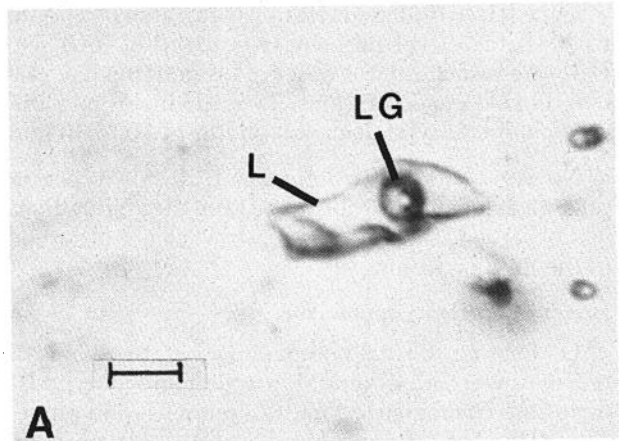

FIG. 6.   Types of primary fluid inclusions in auriferous quartz. Microphotographs are under plane-polarized light, scale = 1 μm. A. Type I inclusion of aqueous liquid phase (L) and liquid + gas CO_2 phases (LG). B. Type II inclusion of liquid CO_2 phase (L). C. Type III inclusion of aqueous liquid phase (L) and gas H_2O or CO_2-H_2O phase (G).

Type III: two-phase inclusions of an aqueous liquid with 10 to 50 vol percent H_2O gas (Fig. 6C). No clathrate formation was observed, signifying low carbon dioxide concentrations. Type III inclusions, the least abundant type, have top widths of 10 to 30 μm.

No systematic distribution of inclusion types in relation to location within or between the vein systems was observed. Daughter minerals were not observed in the fluid inclusions.

Homogenization phenomena

On heating to total homogenization, two kinds of behavior were observed. Most type I and all type III inclusions homogenized in the aqueous liquid phase. The CO_2 phase in type I and the H_2O-gas phase in type III gradually diminished in volume, moved vigorously within the inclusion cavity, and then disappeared at a temperature presumed to be the homogenization point. A second type of behavior was observed in some type I inclusions, whereby the CO_2 phase diminished in size on initial heating and then maintained a uniform size through most of the heating. The miniscus then became hazy, and at a temperature a few degrees higher, disappeared without any appreciable change in size.

Homogenization temperatures of type I inclusions range from 220° to 360°C, and type III ones from 120° to 220°C (Fig. 7, Table 3). Assuming the fluids were homogeneous at time of entrapment in the host quartz, the range of temperatures indicates a range in trapping temperature, trapping pressure, salinity, or any combination of the three (Roedder, 1979; Roedder and Bodnar, 1980). If the assumption is not true and fluids consisted of immiscible phases, then the homogenization data are difficult to interpret.

Many type I inclusions when heated decrepitated. The inclusions darkened and a gas of low refractive index filled the cavity and its peripheral microcracks. Decrepitation results from the isochoric rise in inter-

nal pressure, as the inclusion is heated, to a point exceeding the strength of the cavity wall (Roedder, 1979). Decrepitation temperatures cluster around the two homogenization peaks, at 229° ± 3.8°C for eight measurements and 271° ± 4.5°C for ten measurements. This observation suggests that inclusions which decrepitated did so at or near their respective homogenization points.

Freezing and melting phenomena

On cooling type I inclusions to about −40°C, the CO_2-laden bubble became oval shaped and reduced in volume; platelike crystals formed, projecting into the outer aqueous phase. After a short time the outline of the distorted bubble became jagged and coarse indicating the formation of clathrate, a carbon dioxide hydrate compound (Collins, 1979; Burruss, 1981b). On further cooling the aqueous phase turned into a granular mass of ice crystals, the CO_2 phase solidified, and the inclusions appeared nearly opaque. For most inclusions this double freezing phenomenon was not completed unless cooling was continued to −80°C. Measuring the temperature of clathrate melting proved difficult due to similar refractive indices of clathrate and aqueous solution. The temperature of disappearance of the jagged interface in the presence of liquid and gas CO_2 was presumed to be the melting temperature of the clathrate (Fig. 8).

On cooling type II inclusions below 0°C, a second phase presumed to be CO_2 gas separated. On further cooling to a temperature as low as −80°C, the liquid CO_2 froze to an irregular crystal aggregate and the CO_2 phase became oval. When the inclusion was slowly heated, the temperature at which the frozen CO_2 began to melt, and liquid CO_2 was observed around the gas bubble, was recorded to be the melting point of CO_2 (Fig. 8). Melting temperatures of solid CO_2 for types I and II average −56.8° ± 0.1°C, signifying nearly pure CO_2, given that the eutectic melting point of CO_2 is −56.6°C (Weast, 1977).

Translucent masses of ice formed when type III inclusions were frozen. On heating before final melting, the gas bubble adhered to the last ice crystal visible, which was in motion inside the inclusion cavity. The end of this motion combined with disappearance of the ice crystal was presumed to be the melting point of the ice (Fig. 8).

Salinity

Figure 9 predicts the curve relation between fluid salinity and the melting points of ice and clathrate. The solute content of the entrapped fluids (Table 3), expressed as an apparent salinity in terms of NaCl equivalent in wt percent (Roedder, 1963), was estimated from the measured melting points of the ice
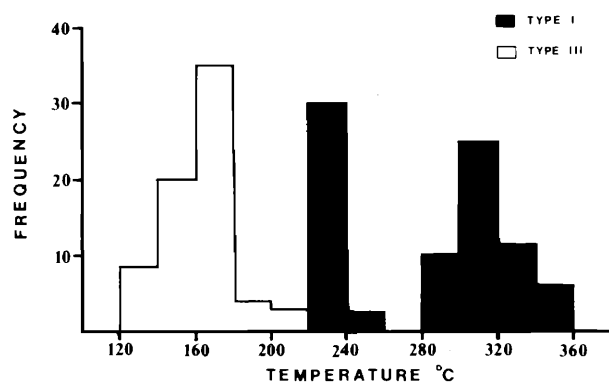

FIG. 7.   Homogenization temperatures of fluid inclusion types.

TABLE 3.   Homogenization Temperature, Apparent Salinity, and Density of Primary Fluid Inclusions[1]

Inclusion types	Homogenization temperature (°C)		Apparent salinity[2] (equiv wt % NaCl)	Density (g/cm^3)[3]	
	Total	CO_2 phase		CO_2 phase	Bulk
I	R: 220–360 X: 232 ± 6.5 X: 311 ± 3.9	R: 15–30 X: 24 ± 2.3	4–8	R: 0.60–0.83 X: 0.75	R: 0.93–1.01 X: 0.97
II		R: 0–10 X: 3.2 ± 1.5	0	R: 0.86–0.96 X: 0.95	
III	R: 120–220 X: 161 ± 25.7		11–14		R: 1.04–1.08 X: 1.06

[1] Data are from Figures 7 and 8; R = range, X = average, ± = standard deviation
[2] For type I, salinity is estimated from the clathrate melting temperature of 7° ± 0.9°C; for type II, salinity is estimated from the eutectic melting point for CO_2 of −56.8° ± 0.1°C; for type III, salinity is estimated from the ice melting point of −9° ± 1.4°C
[3] Density of CO_2 phase derived from CO_2 homogenization temperatures, after Roedder (1965); density of NaCl-H_2O phase at room temperature is taken from Weast (1977); bulk density is estimated from densities and proportions of phases observed in fluid inclusions, after Burruss (1981b)

and clathrate. The presence of salts in the fluid inclusions is evidenced by the depression of the melting points of ice and clathrate from 0°C in pure water for ice and 10°C in pure carbon dioxide-water for clathrate.

Salinity estimates for type III inclusions are probably in error because the effect of dissolved CO_2 in the aqueous phase was neglected. The minimum concentration necessary for liquid CO_2 to form in a fluid inclusion at 10°C is approximately 2.2 molal in pure water and less in a saline solution (Hedenquist and Henley, 1985). At CO_2 concentrations of approximately 0.85 to 2.2 molal, clathrate will form upon cooling of the fluid inclusion (Collins, 1979). In type III inclusions, liquid CO_2 and clathrate formation were not observed, constraining the CO_2 content of the fluid to less than 0.85 molal. Based on the study of Hedenquist and Henley (1985), dissolved CO_2 in type III inclusions could contribute up to −1.5°C to the

total depression of the ice melting point, reducing the salinity estimate by up to 1 equiv wt percent NaCl.

Density

Table 3 presents estimates of CO_2 phase and bulk densities. Density of the CO_2 phase was estimated by plotting the phase's homogenization temperature (Fig. 8) on the experimental solvus of the pure CO_2 system (after Roedder, 1965). Bulk density of each inclusion type was estimated from the densities of the various phases present coupled with visual estimates of the phases' volume proportions at room temperature, assuming an inclusion volume of 1 cm³ (after Burruss, 1981b). For example, type I inclusions with 25 vol percent CO_2 with a density of 0.75 g/cm³ and
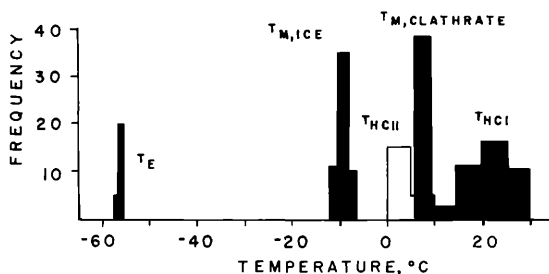

FIG. 8.   Freezing and melting temperatures of fluid inclusion types. T_e is the eutectic temperature of types I and II; $T_{m_{ice}}$ is the ice melting temperature of type III; $T_{m_{clathrate}}$ is the clathrate melting temperature of type I; $T_{h_{CI}}$ is the homogenization temperature of CO_2 phases in type I; $T_{h_{CII}}$ is the homogenization temperature of CO_2 phases in type II.
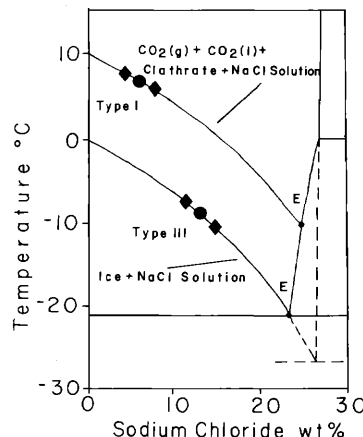

FIG. 9.   Curves for the depression of the melting temperature for clathrate (after Bozzo et al., 1975) and ice (after Roedder, 1962) by sodium chloride.

with 75 vol percent $NaCl-H_2O$ with a density of 1.034 g/cm^3 give the following results:

Bulk density

$$= [(0.75 \, cm^3)(1.034 \, g/cm^3)$$
$$\qquad\qquad + (0.25 \, cm^3)(0.75 \, g/cm^3)]/[1 \, cm^3],$$
$$= [(0.755 \, g) + (0.1875 \, g)]/[1 \, cm^3],$$
$$= 0.96 \, g/cm^3.$$

Interpretation

The major findings of the research are as follows. The spatial association between auriferous quartz veins, calcite-bearing alteration, and abundant CO_2-laden fluid inclusions suggests that type I or II inclusions, or both, are derived from the gold-transporting fluid. The environment in and adjacent to the vein systems was fluid dominated, based on the mineral and chemical alteration of vein wall rocks. Fluid inclusions of types I and II, and of the least abundant type III, coexist in vein quartz and have variable CO_2 to $NaCl-H_2O$ phase proportions and nonuniform homogenization temperatures.

If the primary fluid inclusions experienced no change in volume or constituents after sealing, then two origins are considered likely. First, the fluid inclusions may represent two or three generations of fluids with no obvious paragenesis, entrapped in quartz veins over a range of temperature and pressure. Second, a heterogeneous fluid comprised of immiscible CO_2 and $NaCl-H_2O$ phases may have been entrapped in the crystallizing quartz at time of gold concentration. The mutual solubilities of CO_2 and H_2O change considerably with temperature, pressure, and salinity (Roedder, 1979; Roedder and Bodnar, 1980; Burruss, 1981a, b); water and carbon dioxide are immiscible over a wide field of temperatures and pressures. If a fluid comprised of two or more immiscible phases is trapped in a growing crystal, then the resulting fluid inclusions will in all likelihood have nonuniform phase proportions and total homogenization temperatures.

Conclusions

1. Native gold exists in quartz vein systems with chlorite + white mica + albite + calcite + quartz alteration in Archean granitic rocks near Wawa, Ontario.

2. Alteration of the granitic wall rocks added K, CO_2 + H_2O, Rb and Ba and removed Na, suggesting a fluid-dominated system.

3. Three types of primary fluid inclusions coexist in the quartz veins. Type I, the most abundant type, is an aqueous liquid with 10 to 25 vol percent CO_2

with a density of 0.75 g/cm^3; homogenization temperatures range from 220° to 360°C. Type II is nearly 100 vol percent liquid CO_2 with a density of 0.95 g/cm^3. Type III, the least abundant type, is an aqueous liquid with 10 to 50 vol percent H_2O gas; homogenization temperatures range from 120° to 220°C.

4. Apparent salinities of type I, II, and III inclusions, based on clathrate and ice melting points, are 4 to 8, 0, and 11 to 14 equiv wt percent NaCl, respectively.

5. The gold-bearing quartz veins may be interpreted to have formed from CO_2-laden fluids of less than 10 equiv wt percent NaCl during regional greenschist metamorphism of the Archean granitic rocks.

REFERENCES

Attoh, K., 1980, Stratigraphic relations of the volcanic sedimentary successions in the Wawa greenstone belt, Ontario: Canada Geol. Survey Paper 80-1A, p. 101–106.

Ayres, L. D., 1972, Guide to granitic rock nomenclature used in reports of the Ontario Division of Mines: Ontario Div. Mines Misc. Paper 52, 14 p.

Boyle, R. W., 1979, The geochemistry of lode gold deposits (together with a chapter on geochemical prospecting for the elements): Canada Geol. Survey Bull. 280, 584 p.

Bozzo, A. T., Chen, H. S., Kass, J. R., and Barduhn, A. J., 1975, The properties of the hydrates of chlorine and carbon dioxide: Desalination, v. 16, p. 303–320.

Burruss, R. C., 1981a, Analysis of fluid inclusions: Phase equilibria at constant volume: Am. Jour. Sci., v. 281, p. 1104–1126.

—— 1981b, Analysis of phase equilibria in C-O-H-S fluid inclusions: Mineralog. Assoc. Canada Short Course Handbook, v. 6, p. 39–74.

Collins, P. L. F., 1979, Gas hydrates in CO_2-bearing fluid inclusions and the use of freezing data for estimation of salinity: ECON. GEOL., v. 74, p. 1435–1444.

Gresens, R. L., 1967, Composition-volume relationships of metasomatism: Chem. Geology, v. 2, p. 47–65.

Guha, J., Gauthier, A., Vallee, M., Descarreaux, J., and Lange-Brard, F., 1982, Gold mineralization patterns at the Doyon mine (Silverstack), Bousquet, Quebec: Canadian Inst. Mining Metallurgy Spec. Vol. 24, p. 50–57.

Hedenquist, J. W., and Henley, R. W., 1985, The importance of CO_2 on freezing point measurements of fluid inclusions: Evidence from active geothermal systems and implications for epithermal ore deposition: ECON. GEOL., v. 80, p. 1379–1406.

Hodgson, C. J., and MacGeehan, P. J., 1982, A review of the geological characteristics of 'gold only' deposits in the Superior province of the Canadian Shield: Canadian Inst. Mining Metallurgy Spec. Vol. 24, p. 211–229.

Kerrich, R., 1981, Archean gold-bearing chemical sedimentary rocks and veins: A synthesis of stable isotope and geochemical relations: Ontario Geol. Survey Misc. Paper 97, p. 144–167.

Kerrich, R., and Hodder, R. W., 1982, Archean lode gold and base metal deposits, chemical evidence for metal fractionation into independent hydrothermal reservoirs: Canadian Inst. Mining Metallurgy Spec. Vol. 24, p. 144–160.

Kilias, S., 1984, Genesis of gold deposits, Renabie area, Sudbury district, Ontario: Unpub. M.Sc. thesis, Univ. Ottawa, 210 p.

Krauskopf, K. B., 1967, Introduction to geochemistry: New York, McGraw-Hill, 721 p.

MacDonald, A. J., and Spooner, E. T. C., 1981, Calibration of a Linkam TH 600 programmable heating-cooling stage for microthermometric examination of fluid inclusions: ECON. GEOL., v. 76, p. 1248–1258.

Roedder, E., 1962, Studies of fluid inclusions I: Low temperature application of a dual-purpose freezing and heating stage: ECON. GEOL., v. 57, p. 1045–1061.

—— 1963, Studies of fluid inclusions II: Freezing data and their interpretation: ECON. GEOL., v. 58, p. 167–211.

—— 1965, Liquid CO_2 inclusions in olivine bearing nodules and phenocrysts from basalts: Am. Mineralogist, v. 50, p. 1746–1786.

—— 1979, Fluid inclusions as samples of ore fluids, *in* Barnes, H. L., ed., Geochemistry of hydrothermal ore deposits: New York, Wiley Intersci., p. 684–737.

Roedder, E., and Bodnar, R. J., 1980, Geologic pressure determination from fluid inclusion studies: Ann. Rev. Earth Planet. Sci. Letters, v. 8, p. 263–301.

Sage, R. P., 1981, Preliminary interpretation of the relationship between mineralization and volcanic stratigraphy in the Wawa area: Ontario Geol. Survey Misc. Paper 100, p. 41–44.

Shepherd, T. J., 1981, Temperature-programmable, heating-freezing stage for microthermometric analysis of fluid inclusions: ECON. GEOL., v. 76, p. 1244–1247.

Smith, T. J., Cloke, P. L., and Kesler, S. E., 1984, Geochemistry of fluid inclusions from the McIntyre-Hollinger gold deposit, Timmins, Ontario, Canada: ECON. GEOL., v. 79, p. 1265–1285.

Studemeister, P. A., 1983, The greenschist facies of an Archean assemblage near Wawa, Ontario: Canadian Jour. Earth Sci., v. 20, p. 1409–1420.

Tintor, N., 1984, Drilling at Renabie gets fine deep ore: Northern Miner, v. 70, no. 26, p. A1–A2.

Walsh, J. F., Haynes, F. M., Kesler, S. E., Van Hees, E., and Duff, D., 1984, Fluid inclusion analyses of auriferous vein quartz from the Porcupine District, Ontario [abs.]: Geol. Assoc. Canada-Mineral. Assoc. Canada Program with Abstracts, v. 9, p. 114.

Weast, R. C., ed., 1977, CRC handbook of chemistry and physics: Cleveland, CRC Press, 793 p.